

Pseudorapidity distributions of charged particles from Au+Au collisions at the maximum RHIC energy.

I. G. Bearden⁷, D. Beavis¹, C. Besliu¹⁰, Y. Blyakhman⁶, B. Budick⁶, H. Bøggild⁷, C. Chasman¹, C. H. Christensen⁷, P. Christiansen⁷, J. Cibor³, R. Debbe¹, E. Enger¹², J. J. Gaardhøje⁷, K. Hagel⁸, O. Hansen⁷, A. Holm⁷, A. K. Holme¹², H. Ito¹¹, E. Jakobsen⁷, A. Jipa¹⁰, J. I. Jørdre⁹, F. Jundt², C. E. Jørgensen⁷, R. Karabowicz⁴, T. Keutgen⁸, E. J. Kim¹, T. Kozik⁴, T. M. Larsen¹², J. H. Lee¹, Y. K. Lee⁵, G. Løvholden¹², Z. Majka⁴, A. Makeev⁸, B. McBreen¹, M. Mikelsen¹², M. Murray⁸, J. Natowitz⁸, B. S. Nielsen⁷, J. Norris¹¹, K. Olchanski¹, J. Olness¹, D. Ouerdane⁷, R. Planeta⁴, F. Rami², D. Röhrich⁹, B. H. Samset¹², D. Sandberg⁷, S. J. Sanders¹¹, R. A. Sheetz¹, P. Staszal⁷, T. F. Thorsteinsen⁹⁺, T. S. Tveter¹², F. Videbæk¹, R. Wada⁸, A. Wieloch⁴, and I. S. Zgura¹⁰
(BRAHMS Collaboration)

¹ Brookhaven National Laboratory, Upton, New York 11973, ² Institut de Recherches Subatomiques and Université Louis Pasteur, Strasbourg, France, ³ Institute of Nuclear Physics, Krakow, Poland, ⁴ Jagiellonian University, Krakow, Poland, ⁵ Johns Hopkins University, Baltimore, Maryland 21218, ⁶ New York University, New York, New York 10003, ⁷ Niels Bohr Institute, University of Copenhagen, Denmark, ⁸ Texas A&M University, College Station, Texas 77843, ⁹ University of Bergen, Department of Physics, Bergen, Norway, ¹⁰ University of Bucharest, Romania, ¹¹ University of Kansas, Lawrence, Kansas 66049, ¹² University of Oslo, Department of Physics, Oslo, Norway, ⁺ *Deceased*
(Dated: Version: dndeta200-draft40.tex, Nov. 28, 2001)

We present charged particle densities as a function of pseudorapidity and collision centrality for the $^{197}\text{Au}+^{197}\text{Au}$ reaction at $\sqrt{s_{NN}}=200$ GeV, the maximum energy for RHIC. The charged particle multiplicity for the 5% most central events is 625 ± 1 (stat) ± 55 (syst), i.e. a 14% increase relative to $\sqrt{s_{NN}}=130$ GeV collisions. The total multiplicity of charged particles for $-4.7 \leq \eta \leq 4.7$ is 4630 ± 370 , an increase by 21% over the lower energy. The data show an increase from 2.9 to 3.7 in the production of charged particles per pair of participant nucleons from peripheral (40-50%) to central (0-5%) collisions around midrapidity. These results constrain current models based on high density QCD gluon saturation and on the superposition of particle production from soft hadronic and hard partonic collisions.

PACS numbers: 25.75.Dw

A central question in the study of collisions between heavy nuclei at the maximum energy of the RHIC facility, $\sqrt{s_{NN}}=200$ GeV, is the role of hard scatterings between partons and the interactions of these partons in a high-density environment. Indeed, it has been conjectured that new phenomena related to non-perturbative QCD may come into play at this energy. Among these, a saturation of the number of parton (mainly gluon) collisions in central nucleus-nucleus collisions has been predicted to limit the production of charged particles [1, 2, 3]. Recently, indications for a reduction in the number of hadrons at high transverse momentum for $\sqrt{s_{NN}}=130$ GeV collisions have been presented that may hint at suppression of hadronic jets at high matter densities [4, 5].

The present Letter addresses these issues with the first comprehensive investigation of multiplicity distributions of emitted charged particles in relativistic heavy-ion collisions between ^{197}Au at 100A GeV + 100A GeV. In particular, we have measured pseudorapidity distributions of charged particles in the range $-4.7 \leq \eta \leq 4.7$ for such collisions at $\sqrt{s_{NN}}=200$ GeV as a function of collision centrality. The production of charged particles in these highly energetic nuclear collisions can be due to hadronic as well as partonic collision processes and thus depends

on the presence of gluon shadowing effects and, in general, on the relative importance of soft and hard scattering processes. We find that the production of charged particles at midrapidity increases by $(14 \pm 1)\%$ for the most central collisions relative to $\sqrt{s_{NN}}=130$ GeV collisions [6, 7, 8, 9], in agreement with the results of the PHOBOS experiment [10]. We also observe an increase in particle production with energy for more peripheral collisions. In addition, a saturation of the excitations at larger rapidities is seen for all centralities.

The BRAHMS experiment consists of two magnetic spectrometers for measuring spectra of identified charged particles over a wide range of rapidity and transverse momentum and a number of global detectors for determining the location of the collision vertex, the time of the collision, the collision centrality and the charged particle densities [11]. The present data were obtained using three of the global detector systems at BRAHMS: the Multiplicity Array (MA), the Beam-Beam Counter arrays (BBC), and the Zero-Degree Calorimeters (ZDC). An analysis of charged particle densities for Au+Au reactions at $\sqrt{s_{NN}}=130$ GeV that is very similar in method to that presented here is described in ref. [9].

The MA determines charged particle densities around midrapidity and consist of a double, hexagonal-sided bar-

rel arrangement with a modestly segmented Si strip detector array (SiMA) surrounded by an outer plastic scintillator tile array (TMA). Each of the 25 Si detectors (4 cm x 6 cm x 300 μ m), placed 5.3 cm from the beam axis, is subdivided into seven active strips. The TMA was comprised of 35 plastic scintillator tiles (12 cm x 12 cm x 0.5 cm) located 13.9 cm from the beam axis. The effective coverage of the array is $-3.0 \leq \eta \leq 3.0$. Particle densities are deduced from the observed energy loss in the SiMA elements using GEANT simulations [12] to relate energy loss to the number of particles hitting a given detector element [9].

The BBC Arrays consist of two sets of Cherenkov UV-transmitting plastic radiators coupled to photomultiplier tubes. They are positioned around the beam pipe on either side of the nominal interaction point at a distance of 2.20 m. The time resolution of the BBC elements permits the determination of the interaction point with an accuracy of ≈ 0.9 cm. Charged particle multiplicities in the pseudorapidity range $2.1 \leq |\eta| \leq 4.7$ are deduced from the number of particles hitting each detector, as found by dividing the measured ADC signal by that corresponding to a single particle hitting the detector.

The ZDC detectors are located ± 18 m from the nominal interaction vertex and measure neutrons that are emitted at small angles with respect to the beam direction [13]. Clean selection of minimum-biased events required a coincidence between the two ZDCs and a minimum of 4 “hits” in the TMA and is estimated to include 95% of the nuclear reaction cross section. The ZDCs also locate the interaction point with an accuracy of ≈ 3.6 cm.

Reaction centrality is determined by selecting different regions in the total multiplicity distribution in either the MA or BBC arrays. In analyzing particle densities in $dN_{ch}/d\eta$, the centrality dependence of the MA and BBC distributions are based on the total multiplicity measurements of the corresponding array. In the pseudorapidity range of $3.0 \leq \eta \leq 4.2$, where it was possible to analyze the BBC data using both centrality selections, the two analyses give identical results to within 2%. In general, statistical errors on the measurements are less than 1%, while we estimate that the systematic errors are 8% and 10% for the SiMA and BBC arrays, respectively.

Fig. 1 shows the measured pseudorapidity distributions for charged particles for several centrality cuts. The $dN_{ch}/d\eta$ values for these cuts at $\eta=0, 3.0, 4.5$ are listed in Table I, together with the number of participating baryons, N_{part} , estimated from the HIJING model. For the most central collisions (0-5%) the charged particle density reaches $dN_{ch}/d\eta = 625 \pm 55$ at midrapidity. This corresponds to 3.7 ± 0.3 charged particles per participating baryon pair and indicates a $(14 \pm 1)\%$ increase relative to Au+Au reactions at $\sqrt{s_{NN}}=130$ GeV [9, 14]. By integrating the 0-5% multiplicity distribution we deduce that 4630 ± 370 charged particles are emitted in the considered rapidity range. This value is $(21 \pm 1)\%$ higher than at $\sqrt{s_{NN}}=130$ GeV [9]. More detailed inspection shows that the distributions at the two energies are quite similar in

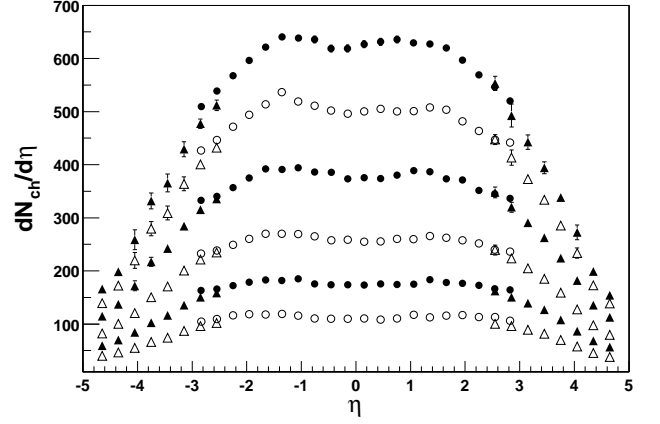


FIG. 1: Distributions of $dN_{ch}/d\eta$ for centrality ranges of, top to bottom, 0-5%, 5-10%, 10-20%, 20-30%, 30-40%, and 40-50%. The SiMA and BBC results are indicated by the circles and triangles, respectively. Statistical error are shown for all points where larger than the symbol size. Systematic errors are 8% and 10% for the SiMA and BBC points respectively.

shape. Indeed, the FWHM of the most central distributions are $\Delta\eta = 7.2 \pm 0.8$ and 7.5 ± 0.5 at $\sqrt{s_{NN}}=130$ GeV and 200 GeV, respectively. For the most peripheral collisions analyzed here (40-50%) the density at $\eta = 0$ is $dN_{ch}/d\eta = 110 \pm 10$ or, scaled to the number of participating pairs, 2.9 ± 0.3 . For comparison, the similar number for $p\bar{p}$ collisions at this energy is 2.5 [15], also a 14% increase over the interpolated lower energy value for $p\bar{p}$ collisions [16].

TABLE I: Charged particle densities in $dN_{ch}/d\eta$ as a function of centrality and pseudorapidity. Total uncertainties, dominated by the systematics, are indicated. The average number of participants $\langle N_{part} \rangle$ and collisions $\langle N_{coll} \rangle$ is given for each centrality class. N_{ch} is the integral charged particle multiplicity within $-4.7 \leq \eta \leq 4.7$.

Cent- rality	$\eta = 0$	$\eta = 1.5$	$\eta = 3.0$	$\eta = 4.5$	N_{ch}	N_{coll}	N_{part}
0-5	625 ± 55	627 ± 54	470 ± 44	181 ± 22	4630 ± 370	936	346
5-10	501 ± 44	515 ± 48	397 ± 37	156 ± 18	3810 ± 300	733	293
10-20	377 ± 33	386 ± 35	309 ± 28	125 ± 14	2920 ± 230	511	228
20-30	257 ± 23	267 ± 23	216 ± 17	90 ± 10	2020 ± 160	317	164
30-40	174 ± 16	182 ± 16	149 ± 14	64 ± 7	1380 ± 110	189	114
40-50	110 ± 10	115 ± 11	95 ± 9	43 ± 5	890 ± 70	103	76

Alternatively, Fig. 2 shows that the charged particle multiplicities in an interval of approximately 0.5-1.5 units below the beam rapidity are independent of the collision centrality and energy, from CERN-SPS energy ($\sqrt{s_{NN}}=17$ GeV) [17] to the present RHIC energy. This is consistent with a limiting fragmentation picture in which the excitations of the fragment baryons saturate already at moderate collision energies independently of the system size [9]. In contrast, the increased projectile kinetic energy is utilized for particle production in the region around midrapidity, as evidenced by the observed

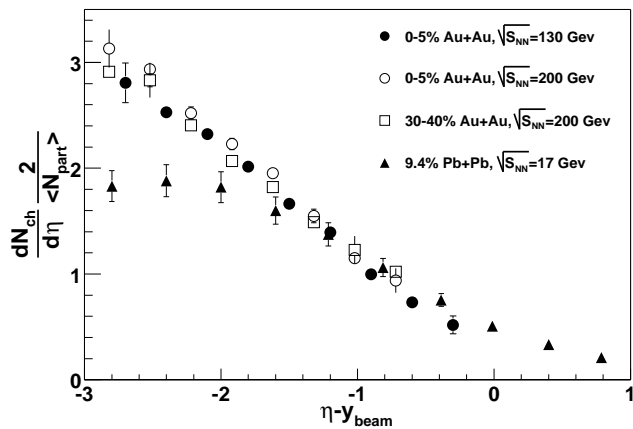


FIG. 2: Charged particle densities normalized to the number of participant pairs (see table) for the present 0-5% central (open circles) and 40-50% central (open squares) Au+Au results at $\sqrt{s_{NN}}=200$ GeV, the BRAHMS Au+Au results [9] at $\sqrt{s_{NN}}=130$ GeV (closed circles) and the 9.4% central Pb+Pb data at $\sqrt{s_{NN}}=17$ GeV (closed triangles) of ref [17]. Data at different beam energies are plotted as a function of the pseudorapidity shifted by the relevant beam rapidity. Representative total uncertainties are shown for a few Au+Au points.

increase of the multiplicities per participant pair around the center of mass rapidity.

Figure 3 presents the $dN_{ch}/d\eta$ distributions obtained averaging the negative and positive halves of the measured distributions to further decrease errors. The solid lines are calculations using the model of Kharzeev and Levin [3] which is based on a classical QCD calculation using parameters fixed to the $\sqrt{s_{NN}}=130$ GeV data. This approach is able to reproduce the magnitude and shape of the observed multiplicity distributions quite well. The dashed lines are the results of calculations with the AMPT model [18, 19, 20], which is a cascade model based on HIJING [21] but including final-state rescattering of produced particles. The AMPT model is also able to account for the general trend of the measured distributions, particularly for the most central collisions. We also plot the similar distributions [15] from $p\bar{p}$ collisions at $\sqrt{s}=200$ GeV, scaled by the corresponding number of Au+Au participant pairs, for the 0-5% and 40-50% centralities. For central collisions the Au+Au data shows a strong enhancement over the entire pseudorapidity range relative to $p\bar{p}$ with an excess of $48 \pm 9\%$ observed a mid-rapidity. This suggests significant medium effects. The observed enhancement decreases to about 10% for 40-50% centrality collisions. We note that the measured distributions show a small increase in width with decreasing centrality, with $\sigma_{RMS} = 2.33 \pm 0.02$ and 2.40 ± 0.02 for the 0-5% and 40-50% centralities, respectively, which can be compared to $\sigma_{RMS} = 2.38 \pm 0.05$ for the $p\bar{p}$ data.

The ratio of the pseudorapidity densities measured at $\sqrt{s_{NN}}=130$ GeV and $\sqrt{s_{NN}}=200$ GeV for different centralities are shown in Fig. 4. An increase in charged particle density as a function of energy for a central plateau

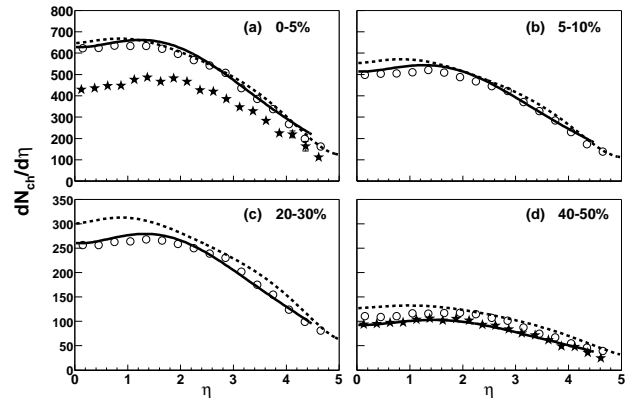


FIG. 3: (a-d) Measured $dN_{ch}/d\eta$ distributions for centrality ranges of 0-5%, 10-20%, 20-30% and 40-50%. Theoretical predictions by Kharzeev and Levin (solid line) and by the AMPT model (dashed line) are also shown. Result from $p\bar{p}$ collisions at this energy [15], scaled by the Au+Au values of $N_{part}/2$, are shown with stars (a,d).

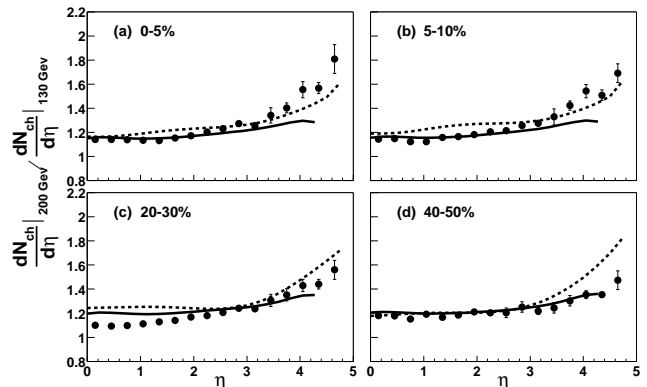


FIG. 4: Ratio of particle densities at $\sqrt{s_{NN}}=200$ GeV and 130 GeV compared to the models. Points are only shown with statistical errors as systematic errors tend to cancel out

region ($|\eta| < 2.5$) is observed, with a comparable increase of between 10% and 20% observed at all centralities. The upturn of the ratios at the forward rapidities is due to the widening of the multiplicity distribution at the higher energy consistent with the increase in beam rapidity ($\Delta y = 0.45$). The overlaid curves show the corresponding ratios resulting from the two model calculations.

Finally in Fig. 5 we plot the dependence of the multiplicity of charged particles per pair of participant baryons as a function of the number of participants N_{part} for three narrow pseudorapidity regions ($\Delta\eta \approx 0.2$) around $\eta = 0$, 3.0 and 4.5. While the figure shows that particle production per participant pair is remarkably constant and near unity at the forward rapidities characteristic of the fragmentation region, this is not the case for the central rapidities. Indeed, we find a significant increase of particle production per pair of participant nucleons for

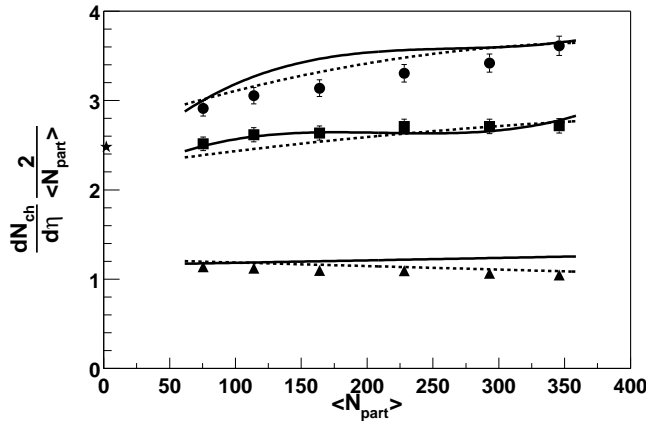


FIG. 5: Distributions of $dN_{ch}/d\eta$ per participant pair as a function of the number of participants (see table) for $\eta = 0, 3.0$ and 4.5 . The curves show predictions by Kharzeev and Levin (solid line) and the AMPT model (dashed line). The star denotes the $p\bar{p}$ result at $\eta = 0$ [15].

the more central collisions at $\eta = 0$. Plotted using the N_{part} values listed in Table 1, the curves for these rapidities rise as a function of collision centrality. This has previously been attributed to the onset of hard scatterings which are dependent on the number of binary nucleon collisions N_{coll} rather than N_{part} . Using N_{coll} values from HIJING [21] we fit the observed dependencies to a functional $dN_{ch}/d\eta = \alpha \cdot N_{part} + \beta \cdot N_{coll}$. For $\eta = 0(4.5)$ we obtain: $\alpha = 1.12 \pm 0.09$ (0.62 ± 0.03) and $\beta = 0.24 \pm 0.04$ (-0.03 ± 0.01). For comparison we find $\alpha = 0.97 \pm 0.08$ (0.50 ± 0.02) and $\beta = 0.22 \pm 0.04$ (-0.07 ± 0.01) at $\sqrt{s_{NN}}=130$ GeV. At $\eta = 0$ we find that the hard scattering component to the charged particle production remains almost constant, with values of $36 \pm 6\%$ and $37 \pm 6\%$ at $\sqrt{s_{NN}}=130$ GeV and 200 GeV, respec-

tively. It should be noted that this analysis of the onset of hard scattering is highly model dependent. Using the N_{part} values from [22], which are smaller than the corresponding HIJING numbers for the more peripheral collisions, the curves of Fig. 5 become essentially flat ($\beta \approx 0$) and thus inconsistent with a mixing of soft and hard scatterings.

In conclusion, we find that the charged particle production scales smoothly from $\sqrt{s_{NN}}=130$ GeV to $\sqrt{s_{NN}}=200$ GeV in a wide region around midrapidity. The data are well reproduced by calculations based on high density QCD and by the AMPT/HIJING microscopic parton model. A phenomenological two-component analysis in terms of a superposition of soft and hard scattering particle production also accounts well for the data but does not show significant differences between the two energies. We find good consistency with the gluon saturation model of Kharzeev and Levin, but stress that within errors of models and data alike, the data can be equally well reproduced by other models not requiring parton-collision saturation. While the current work establishes a baseline for particle production at the maximum energy available for nucleus-nucleus collisions for several years to come, the full understanding of these energetic collisions must await more detailed analyses of hadronic and leptonic observables over a wide region of phase space and rapidity.

We thank the RHIC collider team for their efforts. This work was supported by the Division of Nuclear Physics of the U.S. Department of Energy, the Danish Natural Science Research Council, the Research Council of Norway, the Polish State Committee for Scientific Research (KBN) and the Romanian Ministry of Research. We are grateful to Drs D. Kharzeev E. Levin, Zi-Wei Lin, and H. Heiselberg for useful discussions and model calculations.

-
- [1] L. V. Gribov, E. M. Levin and M. G. Ryskin, Phys.Rep. **100**, 1 (1983).
 - [2] K. J. Eskola, K. Kajantie and K. Tuominen, Phys. Lett. **B497**, 39 (2001).
 - [3] D. Kharzeev and E. Levin, nucl-th/0108006 and private communication.
 - [4] K. Adcox *et al.*, subm. to Phys. Rev. Lett. (2001), nucl-ex/0109003.
 - [5] J. C. Dunlop *et al.*, Nucl. Phys. **A698**, 515c (2002), and B. Lasiuk, *Workshop on High p_T Phenomenon at RHIC*, BNL (2002), unpublished.
 - [6] B. B. Back *et al.*, Phys. Rev. Lett. **85**, 3100 (2000).
 - [7] C. Adler *et al.*, Phys. Rev Lett. **87**, 112303 (2001)
 - [8] K. Adcox *et al.*, Phys. Rev. Lett. **86**, 3500 (2001).
 - [9] I. G. Bearden *et al.*, Phys. Lett. B523 (2001) 227; nucl-ex/0108016.
 - [10] B. B. Back *et al.*, submitted. to Phys. Rev. Lett.(2001), nucl.exp/0108009.
 - [11] I. G. Bearden *et al.*, submitted to Nucl. Inst. Meth A. (2001).
 - [12] GEANT 3.2.1, CERN program library.
 - [13] C. Adler *et al.*, Nucl. Inst. Meth. **A470**, 488 (2001).
 - [14] We have reanalyzed our earlier $\sqrt{s_{NN}}=130$ GeV data to only include the same set of global detectors as used here.
 - [15] G. J. Alner *et al.*, Zeit. Phys. C **33**, 1 (1986).
 - [16] F. Abe *et al.*, Phys. Rev. D **41**, 2330(1990).
 - [17] P. Deines-Jones *et al.*, Phys. Rev. C **62**, 014903(2000).
 - [18] Bin Zhang, C. M. Ko, Bao-An Li and Zi-wei Lin, Phys. Rev. C **61**, 067901 (2001).
 - [19] Zi-wei Lin, Subrata Pal, C. M. Ko, Bao-An Li and Bin Zhang, Phys. Rev. C **64**, 011902R (2001).
 - [20] Zi-wei Lin, Subrata Pal, C.M. Ko, Bao-An Li and Bin Zhang, Nucl. Phys. **A698**, 375c-378c (2002), nucl-th/0105044; and Zi-wei Lin, private communication.
 - [21] X. N. Wang and M. Gyulassy, Phys. Rev. D **44**, 3501 (1991).
 - [22] D. Kharzeev and M. Nardi. Phys. Lett. **B507**, 121 (2001).